

# Electrochemical modeling of lithium polymer batteries<sup>☆</sup>

Dennis W. Dees<sup>a,\*</sup>, Vincent S. Battaglia<sup>a</sup>, André Bélanger<sup>b</sup>

<sup>a</sup>*Electrochemical Technology Program, Chemical Technology Division, Argonne National Laboratory,  
9700 S. Cass Avenue, Argonne, IL 60439 USA*

<sup>b</sup>*Expertise, chimie et matériaux, Direction principale-Recherche et développement-IREQ,  
Institut de recherche d'Hydro-Québec, 1800, boul. Lionel Boulet, Varennes, Que., Canada J3X 1S1*

## Abstract

An electrochemical model for lithium polymer cells was developed and a parameter set for the model was measured using a series of laboratory experiments. Examples are supplied to demonstrate the capabilities of the electrochemical model to obtain the concentration, current, and potential distributions in lithium polymer cells under complex cycling protocols. The modeling results are used to identify processes that limit cell performance and for optimizing cell design. Extension of the electrochemical model to examine two-dimensional studies is also described.

© 2002 Elsevier Science B.V. All rights reserved.

*Keywords:* Lithium; Battery; Electrochemical; Modeling; Polymer

## 1. Introduction

Electrochemical modeling, as described by Newman, has been applied to a number of battery technologies over the last several decades [1]. The method can be used to identify the processes that limit cell performance and offers tremendous predictive capabilities for optimizing cell design. It is a useful tool to help guide research activities and complements experimental cell and component characterization studies. The present effort on the electrochemical modeling of lithium polymer batteries is an ongoing example of how this method can be applied to advanced battery technologies.

In general, electrochemical modeling is used to describe the mass, energy, and momentum transport of each specie for each phase and component of the cell. For battery technologies, the volume-averaged forms of the transport equations are often used because one or both of the electrodes have a composite (multiphase) structure [2,3]. The kinetics and thermodynamics of the chemical and electrochemical reactions are also included. The electrochemical

model typically ends up as a system of coupled partial differential equations that must be solved in time for all the spatial dimensions needed. Electrochemical modeling is not only able to predict macroscopic quantities such as the cell voltage and current, but also the local distribution of concentration, potential, current, and temperature inside the cell on a microscopic scale. Considering the thickness of today's advanced battery systems, these microscopic distributions would be extremely difficult to obtain by any other technique.

Because electrochemical models for complete cells tend to be relatively complex, they typically have many parameters that must be determined. While it is possible in many cases to glean from the literature reasonable estimates of these parameters, to realize the full potential of the model, the parameters must be determined independently to the extent that they can. This is done through a series of experiments that examines the various components of the cell.

The Electrochemical Technology Program at Argonne National Laboratory has been working with the United States Advanced Battery Consortium (USABC) and Hydro-Québec (HQ) since the early 1990s in support of the development of lithium polymer batteries for electric vehicle applications [4,5]. This lithium polymer battery technology is a lightweight high energy and power system that operates at moderate temperatures (typically 50–100 °C). With a polymer electrolyte, this all-solid-state system can be manufactured using high-speed film-laminate technology. While there are a number of current and thermal distribution issues that have been examined in integrating

<sup>☆</sup>The submitted manuscript has been created by the University of Chicago as Operator of Argonne National Laboratory (“Argonne”) under Contract No. W-31-109-ENG-38 with the US Department of Energy. The US Government retains for itself, and others acting on its behalf, a paid-up, non-exclusive, irrevocable worldwide license in said article to reproduce, prepare derivative works, distribute copies to the public, and perform publicly and display publicly, by or on behalf of the Government.

\* Corresponding author. Tel.: +1-630-252-7349.  
E-mail address: dees@cmt.anl.gov (D.W. Dees).

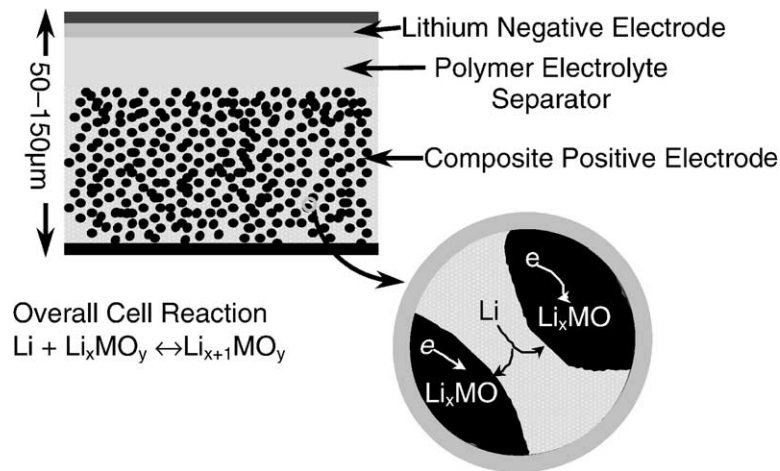


Fig. 1. Diagram of lithium polymer cell with polymer electrolyte separator and a composite positive electrode (vanadium oxide, carbon, and polymer electrolyte).

this thin-film high-surface-area battery technology into full size modules and packs, this modeling effort concentrates on the electrochemically active materials between the current collectors under isothermal conditions.

These active materials, as shown in Fig. 1, consist of a polymer electrolyte separator sandwiched between a metallic lithium negative electrode and a composite positive electrode. While numerous candidate polymer electrolytes have been examined under this program, the present study was aimed at a binary lithium salt (i.e.  $\text{LiN}(\text{CF}_3\text{SO}_2)_2$ ) dissolved in a dry polyether copolymer. The composite electrode is made of a mixture of polymer electrolyte, a conductive carbon additive, and vanadium oxide.

## 2. Model description and development

The electrochemical model for simulating a lithium polymer cell, developed in the present study, builds on the earlier work of Doyle et al. [6]. While the basic model is fundamentally similar, there are differences, described below, which were included for this specific application. They not only include a new set of parameters, but also small variations in the fundamental equations and significant changes in cell operation and geometry. To the extent possible, the model parameters were determined by a series of experiments using specially designed cells and standard cells. Some of these experiments were straightforward to carry out. For example, the open circuit voltage (OCV) as a function of the lithium concentration in the vanadium oxide was determined by a slow ( $\sim C/200$ ) discharge and charge of a cell. Others, such as the polymer electrolyte characterization, required an extensive investigation to establish the parameters.

For the polymer electrolyte and the cell in general the all-solid-state system and assumption of isothermal operation allows the momentum and thermal transport effects to be neglected. The transport equations for the electrolyte then

reduce to mass transfer expressions for each specie (i.e. cation, anion, and polymer solvent) and electroneutrality. In the present model, as in the work of Doyle et al., concentrated solution theory is used to account for the transport of the binary salt in the polymer electrolyte. The polymer electrolyte transport equations used in the present study varied slightly in that they were developed, based on the volume-averaged velocity of the electrolyte [7,8]. The transport parameters (i.e. electrolyte conductivity, salt diffusion coefficient, and cation transference number) and salt activity coefficient for the polymer electrolyte were measured as a function of salt concentration and temperature, through independent studies on symmetric (Li/polymer/Li) cells and concentration cells (Li/polymer<sub>1</sub>/polymer<sub>2</sub>/Li) previously described in [9].

As part of the polymer electrolyte study, the kinetic parameters for the lithium polymer interfacial electrochemical reaction, assuming Butler–Volmer kinetics as described in the work of Doyle et al., was also determined from the AC impedance studies on the symmetric cells. In contrast to the earlier work of Doyle et al., a diffusion overpotential term accounting for the transport of lithium ions through the solid electrolyte interface (SEI) on the lithium electrode was added to the present model. Although, this effect was a relatively small, it was included for completeness based on the AC impedance results. A series of studies using a micro-reference electrode built into the polymer electrolyte separator, as described in the lithium-ion cell study of Amine et al., was used in lithium polymer cells to determine the Butler–Volmer kinetic parameters for the positive electrode active material [10]. As one may expect from the difference in electrochemically active surface area, the contribution to overall cell impedance from the positive electrode kinetics was small when compared with the lithium electrode kinetics. The positive electrode kinetic parameters were, of course, based on an average vanadium oxide particle size determined from cross-sectional images of the positive electrode provided by HQ.

Doyle et al. assumed that the diffusion coefficient for the lithium ions in the positive electrode active material was constant. This assumption allowed them to use a superposition integral to solve for the diffusion in the positive electrode active particles. Numerically, this has the advantage of effectively reducing the problem to a single dimension. While being numerically advantageous, this assumption was physically incorrect for the vanadium oxide active material used in the lithium polymer cells studied. Obtaining reasonable agreement between the model and experiment could only effectively be done with a diffusion coefficient that was a function of lithium concentration in the oxide. Allowing for the concentration dependence of the diffusion coefficient creates a numerical pseudo two-dimensional problem. In the model the distance across the cell was the first dimension and the radial distance of the assumed spherical vanadium oxide particles was the second.

There are a number of options for numerically solving a pseudo two-dimensional problem. For the present study, going to a two-dimensional numerical partial differential equation solver was avoided, because we expected to eventually examine multidimensional applications with the electrochemical model. Instead, the distance across the cell was kept as the first dimension and the oxide particles were radially discretized using a finite difference form of the differential diffusion equation. The lithium concentration at the individual nodes of the oxide particles were then carried as dependent variables in the numerical one-dimensional solver. In the numerical solution of the model, from 2 to 20 nodes were used for the lithium concentration distribution in the oxide particles. After examining the differences in the overall numerical solution, five node points were used to describe the lithium concentration distribution in the oxide particles. Two steps were taken to insure an accurate mass balance of lithium in the oxide particles. First, the actual, rather than the approximate, volume element was used in the finite difference form of the differential diffusion equation. Second, three of the node points were placed close to the surface to accurately account for the surface concentration and flux of lithium ions into and out of the oxide particles.

The diffusion coefficient for the lithium ions in the vanadium oxide particles was determined by fitting the modeling results to constant current charge and discharge experimental studies with lithium polymer cells. This technique is a relatively efficient method to determine the diffusion coefficient, but it is dependent on the model to account for all the other impedance effects in the cell. As mentioned above, a more direct measure of the diffusion coefficient would be preferable, although in this case much more difficult to attain. It is important to realize here that because of the volume averaging in the electrochemical model, the diffusion coefficient for the lithium ions in the vanadium oxide particles is not a fundamental transport parameter of the oxide. It is also dependent on the microstructure of the composite electrode.

For the present application of the model it is important to be able to run the simulation under the same conditions as can be done with experimental lithium polymer cells using today's cyclers. While the model development of Doyle et al. was written for constant current studies, changing the model to also allow for controlled voltage and power applications was relatively straight forward. The total current to the cell was taken as a dependent variable, because it can change with time under controlled voltage and power applications. The boundary conditions were then varied according to what variable was being controlled. For current or voltage control, the respective variable on the boundary can be set directly. If the power is being controlled, then the power would be set equal to the product of the cell current and the cell voltage on the boundary. Setting the external load on the cell can be done in a manner similar to the power, but this option was not implemented in the model.

Besides being able to accept changes in the controlled variable (i.e. current, voltage, or power), the model is also designed to accommodate step changes in the value of the controlled variable. For the model to remain stable through these step changes, the simulation time step has to be reduced and then gradually increased. Thus, many step changes of the controlled variable significantly slows down the calculation. All the changes considered in this study (e.g. cycling, peak power, and dynamic stress test (DST) as defined by the USABC test protocol) range from seconds to hours apart, and the exact voltage profile at times shorter than a second after a change is not critical. Therefore, double-layer charging effects were not included in the electrochemical model.

Mathematically speaking, the electrochemical model is a system of coupled partial differential equations that must be solved in time and space. Two different partial differential equation solvers were used for this purpose. A majority of the work for this study was solved with a program developed by Verbrugge and Gu [11]. The version used was a finite difference based one-dimensional solver that is capable of time stepping. FlexPDE, a finite element three-dimensional partial differential equation solver marketed by PDE Solutions Inc. was used to solve the multidimensional time-dependent current distribution problems.

### 3. Results and discussion

A wide range of simulations was conducted with the electrochemical model of a lithium polymer cell. These investigations generally followed cycling protocols as described in the battery test manuals of the USABC and Partnership for a New Generation of Vehicles (PNGV) [12,13]. Most of the studies conducted and, in fact, all the work presented here are directed towards electric vehicle applications. They include controlled current and power applications using both constant and variable step techniques. While the calculations generally follow actual cell

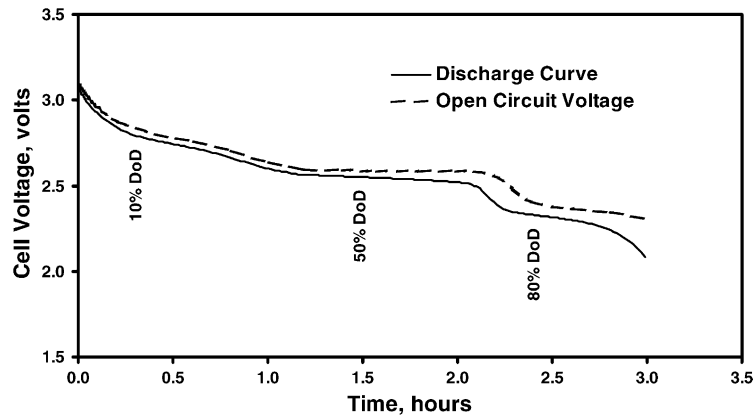


Fig. 2. Simulation of lithium polymer cell during constant current discharge ( $C/3$  rate).

results, all the work presented here is limited to theoretical studies with the electrochemical model.

The discharge curve obtained from the simulation of a lithium polymer cell during a 3 h constant current discharge is given in Fig. 2. At the 3 h rate, the shape of the discharge curve follows that of the cell OCV curve for the first 50% depth-of-discharge (DoD), as indicated in Fig. 2. In the latter stages of discharge, the diffusion coefficient for the lithium ions in the vanadium oxide drops off and eventually becomes the limiting factor at the end of discharge. The vanadium oxide positive electrode active material determines the slope of the OCV curve. As with many intercalation materials, the slope of the OCV curve varies with depth of discharge. These changes in slope affect the current distribution in the positive electrode, as indicated in Fig. 3.

Fig. 3 gives the dimensionless electrochemical reaction rate as a function of a dimensionless cell coordinate in the positive electrode. The average reaction rate for the positive electrode as plotted is one. For the cell coordinate, the electrolyte separator/positive electrode interface is at 0.3 and the positive electrode/current collector interface is at 1.0. For any cell with a composite electrode, the reaction rate distribution in the electrode will be such that it minimizes the overall potential drop through the cell. For the lithium

polymer cells in this study, the chief factors that come into play are the electrolyte and the local open circuit potential on the surface of the oxide. The rate of lithium ion diffusion into the oxide and the slope of the OCV curve determine the change in the local open circuit potential at the surface of the oxide with current. In Fig. 3, the slope of the OCV curve at 10% DoD is steep enough to cause the reaction rate distribution to be relatively uniform. At 50% DoD, the OCV curve changes very little versus DoD. In this region, a wave in the reaction rate distribution travels from the separator side of the positive electrode back to the current collector. At 80% DoD, lithium ion diffusion in the positive electrode material becomes limiting and the reaction rate distribution again becomes uniform.

The discharge curve obtained from the simulation of a lithium polymer cell during a peak power discharge test is given in Fig. 4. As defined by the USABC, a peak power discharge test consists 10 evenly spaced (i.e. 0, 10, 20, ...% DoD) 30 s current pulses applied to the cell during a 3 h controlled current discharge. The drop in cell voltage during each of the current pulses is quite evident. Corresponding to the increased current during the current pulse, there is an increase in the salt concentration gradient in the polymer electrolyte. The salt concentration gradient at the end of the

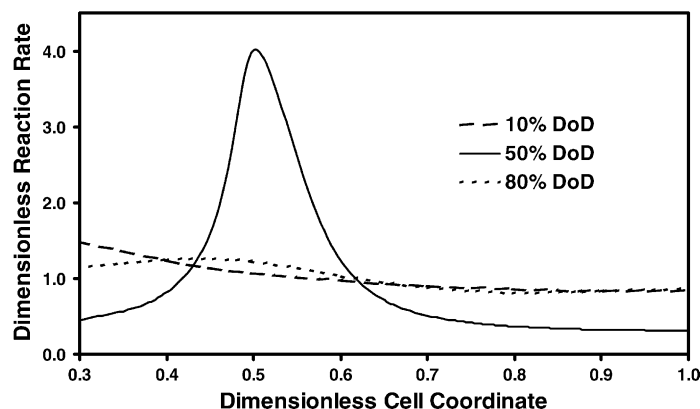


Fig. 3. Current distribution in the positive electrode at 10, 50, and 80% DoD.

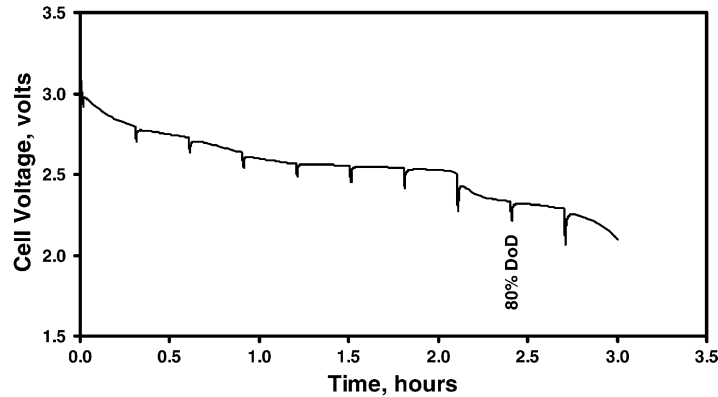


Fig. 4. Simulation of lithium polymer cell during a peak power discharge test.

current pulse increases with the size of the current pulse, as shown in Fig. 5. In Fig. 5, the lithium/polymer interface is at a cell coordinate of zero. As current is passed during discharge, there is a shift in the electrolyte salt from the positive electrode to the separator. Eventually, at high enough current, the salt concentration in the positive electrode can approach zero.

Fig. 6 shows the profile of a controlled power discharge referred to as the DST, as defined by the USABC. The profile not only contains discharge steps, but it also has charging steps representing regenerative braking in an electric vehicle. During the discharge of a cell, the pattern is repeated until the end of discharge has been attained. The simulation of a lithium polymer cell during a DST discharge is shown in Fig. 7. This is a time intensive calculation due to the hundreds of steps involved. An expanded view of the cell voltage and current during a single DST sub-cycle at about 2.6 h into the discharge is given in Fig. 8. Because this is a controlled power discharge, both the current and potential are continuously changing during the discharge. The greatest swing in cell voltage and current occurs between the high discharge steps (i.e. steps 15 and 16) and the high regen step (i.e. step 19).

The local distributions inside the cell can be examined to better understand the effect of these changes in the cell current and voltage during the DST discharge. While the local distribution of each dependent variable at each point in space and time was obtained during the calculation, the focus here is on the end of the highest discharge and regen power steps (i.e. steps 15 and 19) shown in Fig. 8. For the positive electrode, the change in the reaction rate distribution is given in Fig. 9. While it is difficult to extrapolate too much from this comparison, clearly the reaction distribution shifts significantly. Although not as dramatic, the salt concentration distribution in the polymer electrolyte also changes, as shown in Fig. 10. In contrast, the surface lithium concentration on the oxide changes little (see Fig. 11). The relatively long time constant for lithium ion diffusion in the oxide tends to average out the steps applied to the cell.

The observation that the oxide acts as a ballast to help stabilize the fluctuations in the cell can be extended across the complete DST discharge. This behavior is illustrated in Fig. 12, where the average lithium content in the oxide is shown for DST and constant power discharge simulations. The constant power discharge simulation was carried out at the average discharge power for the DST. From a numerical

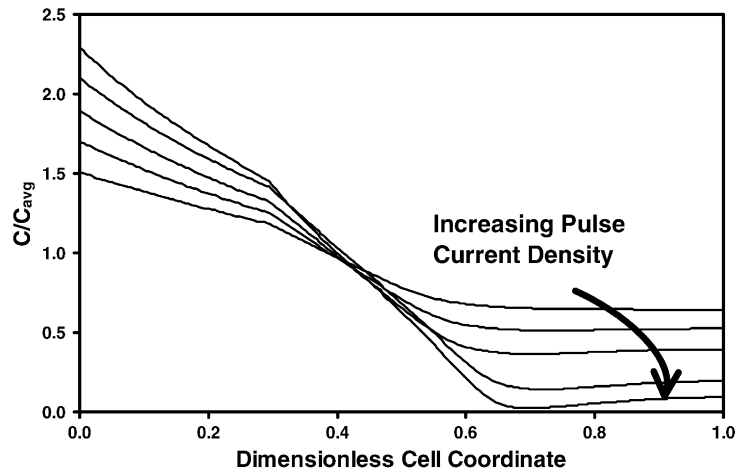


Fig. 5. Increasing salt gradient in polymer electrolyte with peak power pulse current.

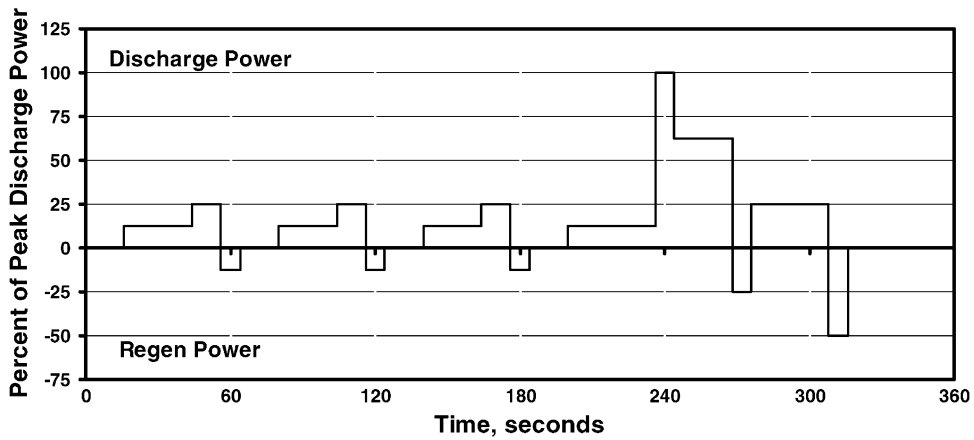


Fig. 6. Cell discharge power control steps for DST driving profile.

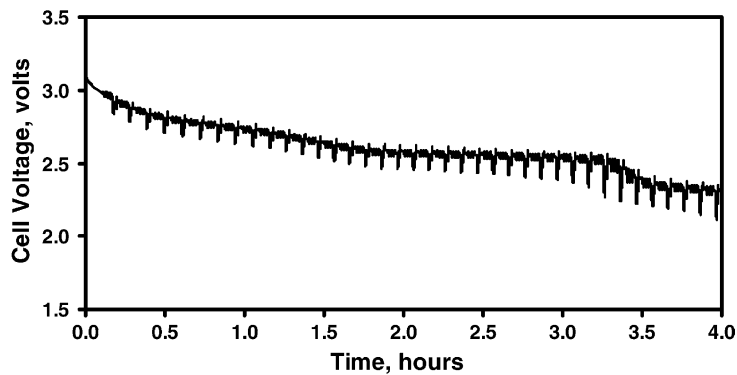


Fig. 7. Simulation of lithium polymer cell during DST discharge.

prospective, this suggests a method of easing the number of calculations for simulating a cell under a DST discharge. For example, it is possible to examine a cell under DST discharge at 80% DoD by running a constant power discharge simulation to within 5 or 10% of the 80% point and then switching over to a DST simulation without sacrificing accuracy.

So far, examples have been given of how electrochemical modeling of lithium polymer cells can be used to examine current, potential, and concentration distributions inside a cell during operation. This information can be used to explain the behavior of macroscopically observed quantities like cell voltage and current. Of possibly even greater significance is that this method can be used to conduct cell

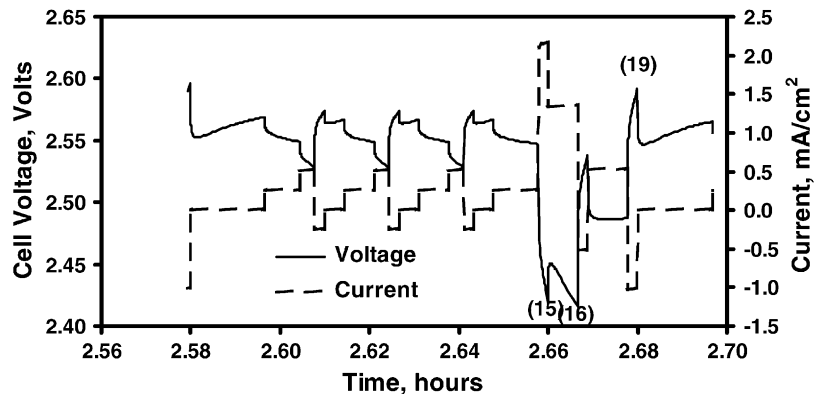


Fig. 8. Simulation of lithium polymer cell during DST discharge sub-cycle (steps 15, 16, and 19 are indicated on graph in parentheses).

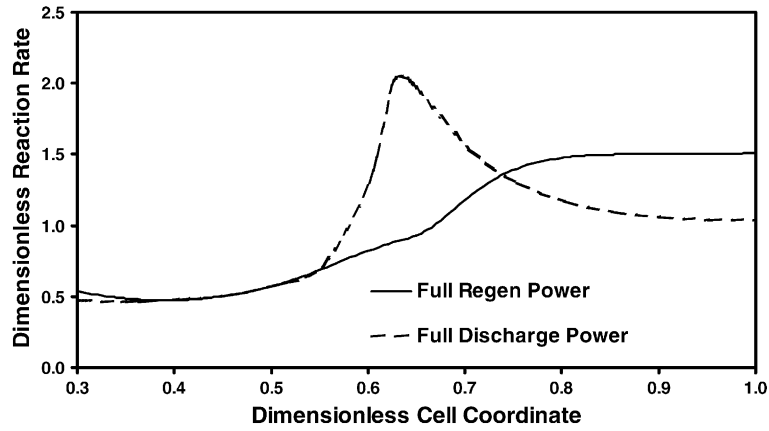


Fig. 9. Current distribution in the positive electrode during DST discharge at the end of the indicated step.

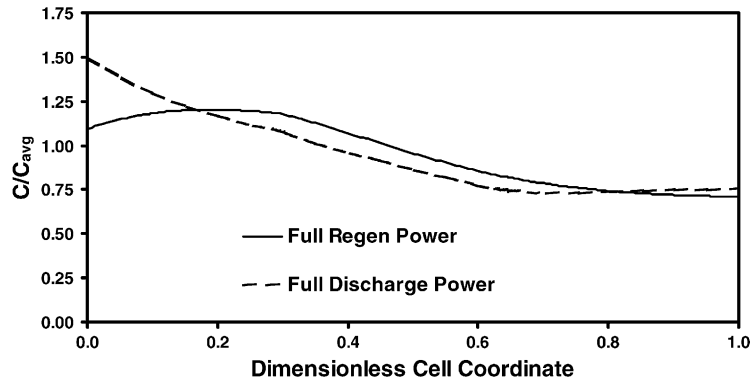


Fig. 10. Salt concentration distribution in the polymer electrolyte during DST discharge at the end of the indicated step.

optimization studies. One example of the many parametric studies that have been conducted is the effect of positive electrode thickness on the cell energy and power. In this work, the specific energy was determined from the simulation of a 3 h discharge and the power was obtained from the simulation of a peak power discharge at 80% DoD. The mass of the electrochemical cell materials (i.e. materials between

the current collectors) was used to calculate the specific energy and power. The electrochemical cell materials include oxide, carbon, polymer electrolyte, and lithium with no excess. Of course, a real cell must have current collectors and other associated hardware, and inclusion of these into the calculations will have a significant impact on the overall result. Using the weight of electrochemical cell materials

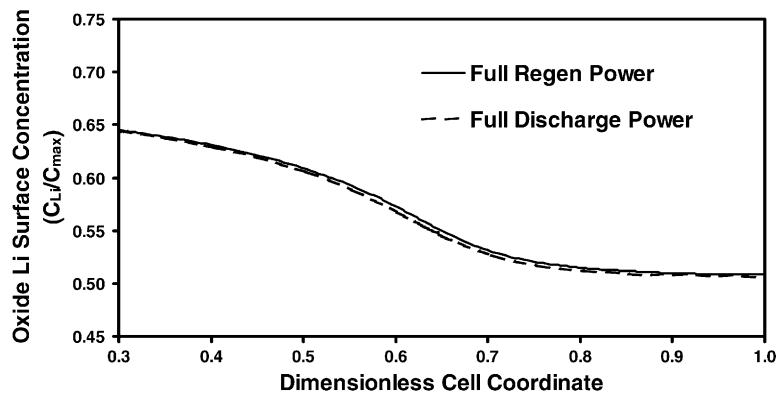


Fig. 11. Lithium concentration distribution on the surface of the vanadium oxide during DST discharge at the end of the indicated step.

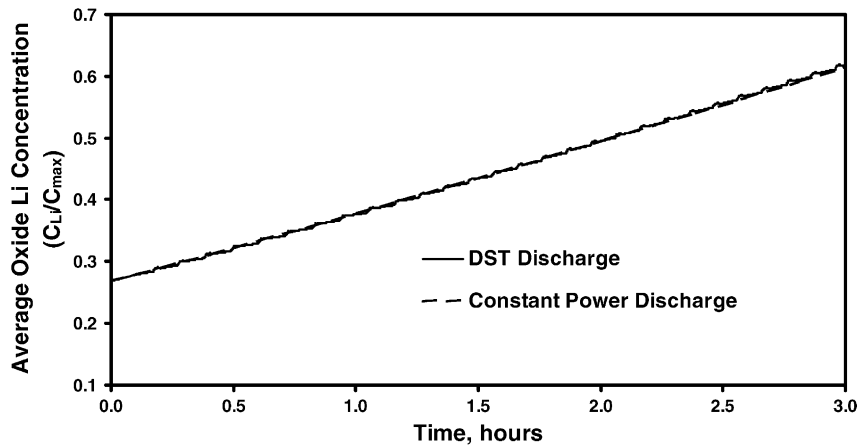


Fig. 12. Simulation of the change in the average lithium concentration in the vanadium oxide for a DST discharge and a constant power discharge at the average power level of the DST.

avoids any discussion of the specifics of the overall cell design and is more than adequate for illustrative purposes.

The calculated specific power of the lithium polymer cell as a function of positive electrode thickness is given in Fig. 13. The positive electrode thickness is reported as an area specific rated capacity (determined from the amount of oxide in the electrode), which is more relevant to battery engineers. When the positive electrode thickness and capacity approach zero, the specific power of the cell also approaches zero for two reasons. First, the mass of the cell remains finite because of the separator. Second, the cell ASI goes to infinity, as shown in Fig. 13. The cell ASI goes to infinity, because the electrochemically active area in the positive electrode is approaching zero with its thickness. As the positive electrode thickness increases from zero, the ASI drops precipitously and the cell specific power increases because of the increase in the electrochemically active area. Eventually, the ASI levels off and even starts to increase slightly. Here another phenomenon becomes significant, namely, the length of the current path in the cell's polymer electrolyte. As the slope of the ASI curve levels out the

specific power drops almost linearly, because mass is being added to the cell with no increase in power.

The calculated specific energy of the lithium polymer cell as a function of positive electrode thickness is given in Fig. 14. As described above, the positive electrode thickness is plotted as area specific rated capacity. When the positive electrode is very thin, the specific energy of the cell approaches zero because the cell energy is approaching zero and the ASI is going to infinity. There is a leveling off of the slope of the specific energy curve because the oxide being added to the cell is getting farther from the lithium electrode and thus, the current path is increasing. This detrimental effect is amplified because a 3 h discharge is being used to calculate the energy; as the positive electrode becomes thicker, the current must correspondingly increase. Comparing the rated capacity and the capacity obtained from the simulation (see Fig. 14) indicates that for the positive electrode thicknesses studied, all of the oxide active material can still be accessed in the 3 h discharge.

While many factors affect the design and performance of a cell, this parametric study does suggest that the lithium

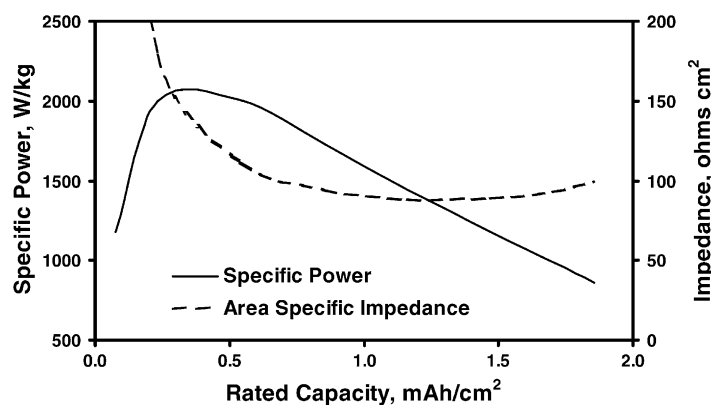


Fig. 13. The calculated specific power and area specific impedance of a lithium polymer cell as a function of positive electrode thickness (plotted as rated capacity).

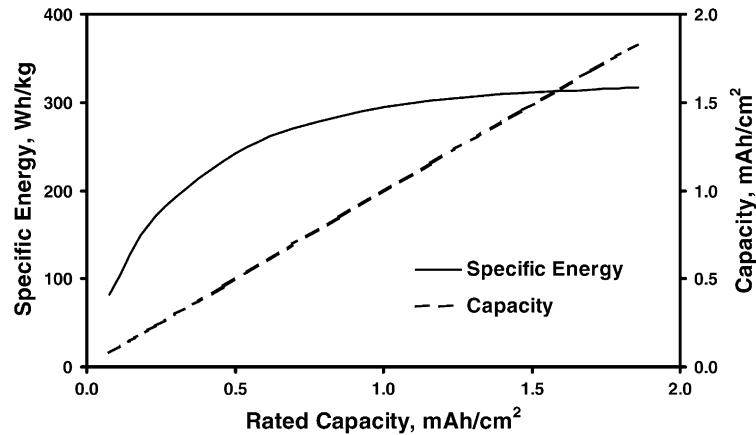


Fig. 14. The calculated specific energy and capacity of a lithium polymer cell as a function of positive electrode thickness (plotted as rated capacity).

polymer technology would be configured differently depending on whether power or energy is more important. For high-power applications, the positive electrode would need to be thinner, and the opposite would be true if energy were the prime motivator. While this conclusion may be intuitive to a battery engineer, these calculations can help serve to narrow the range of interest for a particular application. Alternatively, configurations that may be difficult to attain in the laboratory can be easily examined with the electrochemical model to determine if they should be explored further.

Extending the one-dimensional (not counting lithium ion diffusion in the oxide) electrochemical modeling studies described above to two or even three dimensions allows the current distribution in the cell to be examined further. Specifically, cell imperfections and edge effects can be examined. Also overall cell design issues can be determined, such as the effectiveness of the current collectors to distribute the cell current. Extending the governing equations to

more than one dimension is relatively straightforward, because they were originally developed in three dimensions and then simplified. A current collector for the positive electrode is added to the cell geometry to allow for the total cell current to be set. Without the current collector, a uniform current distribution at the positive electrode/current collector interface must be assumed, which could bias the results of some simulations.

The current distribution, both ionic and electronic, during the simulation of a constant current discharge of a two-dimensional lithium polymer cell is given in Fig. 15. The size and shade of the arrows are indicative of the magnitude of the current, with the darker and larger arrows in each diagram being the greater current. As expected, the ionic current density is uniform in the separator and drops to zero in the positive electrode. In this simulation the ionic current distribution is uniform along all planes parallel to the lithium/polymer electrolyte interface. This is a result of the current collector being conductive enough to

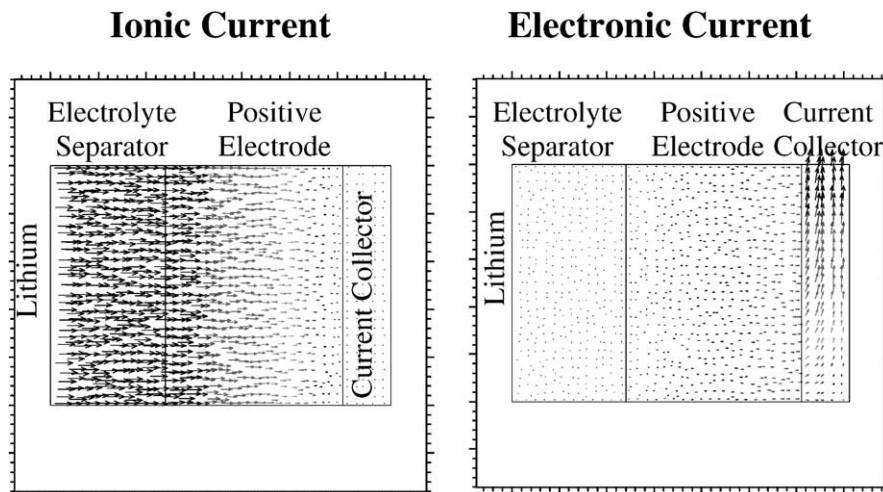


Fig. 15. Ionic and electronic current distributions in lithium polymer cell during a constant current discharge (for each diagram, the darker and larger the arrow, the higher the current density).

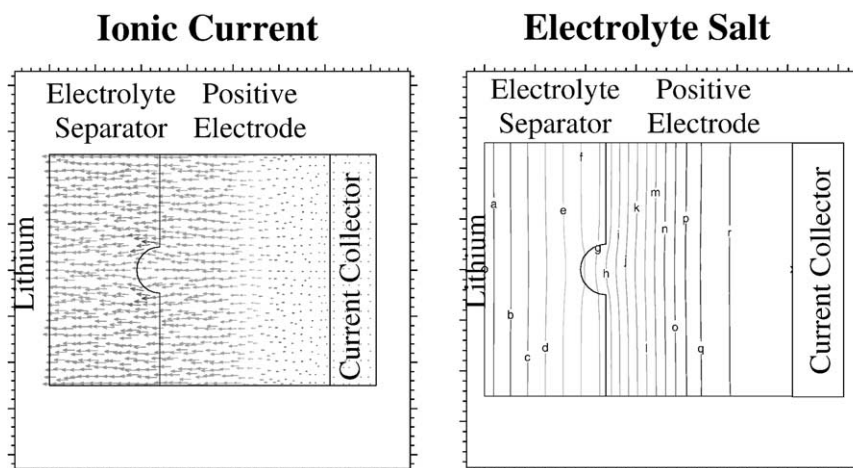


Fig. 16. Ionic current and electrolyte salt concentration distributions during a constant current charge for a lithium polymer cell with an imperfection (for the current diagram, the darker and larger the arrow, the higher the current density. For the salt concentration diagram, the higher the letter the greater the concentration).

uniformly spread out the current to the positive electrode and a featureless geometry. As such, these studies can and have been compared with the one-dimensional work described above, with both PDE solvers yielding essentially the same result. Because of the aspect ratio of the current collector, the maximum electronic current density in the cell is about five times that of the maximum ionic current density.

The utility of a multidimensional electrochemical cell model is only now being fully explored, but an example of how this model can be used is in the study of cell imperfections. Fig. 16 contains the ionic current and polymer electrolyte salt concentration distributions from the simulation of a lithium polymer cell during a constant current charge. The separator/positive electrode interface is non-planar and the current and salt concentration distributions are distorted in the area of the imperfection. However, the overall impact of the imperfection is likely to be small because the distortions do not propagate far from the imperfection. For example, the current distribution on the lithium is relatively uniform.

#### 4. Conclusions

An electrochemical model for lithium polymer cells was developed and a parameter set for the model was measured using a series of laboratory experiments. The electrochemical model was used to identify processes that limit cell performance and for optimizing cell design. Electrochemical modeling was shown to be an effective method for examining concentration, current, and potential distributions in lithium polymer cells. The model was designed to have the capability of following the same cycling protocols required of electric and hybrid electric vehicle battery developers. The information from these studies was used

to understand and explain the behavior of macroscopically observed quantities like cell voltage and current. The predictive capability of electrochemical model was demonstrated by examining the effect of positive electrode thickness on cell power and energy. The implication of using the electrochemical model to conduct parametric studies for the design of a lithium polymer cell in a specific application was exhibited. The electrochemical model development was extended to include two-dimensional studies on lithium polymer cells. All the results presented here were intended to give a flavor of how electrochemical modeling can be applied to advanced battery technologies.

#### Acknowledgements

This work was performed under the auspices of the US Department of Energy, Office of Advanced Automotive Technologies, under contract number W-31-109-ENG-38. The authors gratefully acknowledge the support and guidance of Hydro-Québec and the United States Advanced Battery Consortium.

#### References

- [1] J.S. Newman, *Electrochemical Systems*, Prentice-Hall, Ont., Canada, 1991.
- [2] P. De Vidts, R.E. White, *J. Electrochem. Soc.* 144 (1997) 1343.
- [3] S. Whitaker, *The Method of Volume Averaging*, Kluwer Academic Publishers, Dordrecht, 1999.
- [4] M. Gauthier, A. Belanger, P. Bouchard, B. Kapfer, S. Ricard, G. Vassort, M. Armand, J.Y. Sanchez, L. Krause, *J. Power Sources* 54 (1995) 163.
- [5] C. LeTourneau, M. Gauthier, A. Belanger, D. Kuller, J. Hoffman, Lithium polymer battery pack design, in: *Proceedings of the 14th International Electric Vehicle Symposium and Exposition*, 15–17 December, Orlando, FL, 1997.

- [6] M. Doyle, T. Fuller, J. Newman, *J. Electrochem. Soc.* 140 (1993) 1526.
- [7] R. Pollard, T. Comte, *J. Electrochem. Soc.* 136 (1989) 3734.
- [8] J. Newman, T.W. Chapman, *AIChE J.* 19 (2) (1973) 343.
- [9] D. Dees, V. Battaglia, L. Redey, G. Henriksen, R. Atanasoski, A. Belanger, *J. Power Sources* 89 (2000) 249.
- [10] K. Amine, C. Chen, J. Liu, M. Hammond, A. Jansen, D. Dees, I. Bloom, D. Vissers, G. Henriksen, *J. Power Sources* 97/98 (2001) 684.
- [11] M. Verbrugge, H. Gu, Finite difference routines for one and two-dimensional problems utilizing a functional programming style, in: J. Newman, R. White (Eds.), *Proceedings of the Douglass N. Bennion Memorial Symposium*, The Electrochemical Society, Vol. 94/22, Pennington, NJ, 1994, p. 153.
- [12] USABC Electric Vehicle Battery Test Procedures Manual, Review 2, 1996.
- [13] PNGV Battery Test Manual, DOE/ID-10597, Review 3, 2001.